Earth's Future

Supporting Information for

Projecting Changes in the Drivers of Compound Flooding in Europe Using CMIP6 Models

Tim H.J. Hermans[1], Julius J.M. Busecke[2], Thomas Wahl[3], Víctor Malagón-Santos[4], Michael G. Tadesse[5], Robert A. Jane[3], and Roderik S.W. van de Wal[1,6]

[1]Institute for Marine and Atmospheric Research Utrecht, Utrecht University, Utrecht, The Netherlands

[2]Lamont-Doherty Earth Observatory, Columbia University, Palisades, NY, USA

[3]Civil, Environmental, and Construction Engineering National Center for Integrated Coastal Research, University of Central Florida, Orlando, USA

[4]NIOZ Royal Netherlands Institute for Sea Research, Department of Estuarine Delta Systems, PO Box 140, 4400AC Yerseke, The Netherlands

[5]Hazen and Sawyer, Orlando, FL, USA

[6]Department of Physical Geography, Utrecht University, Utrecht, 3584 CB, The Netherlands

Contents of this file

Introduction

This Supporting Information contains 16 figures supplementary to the main manuscript.

Supporting Figures

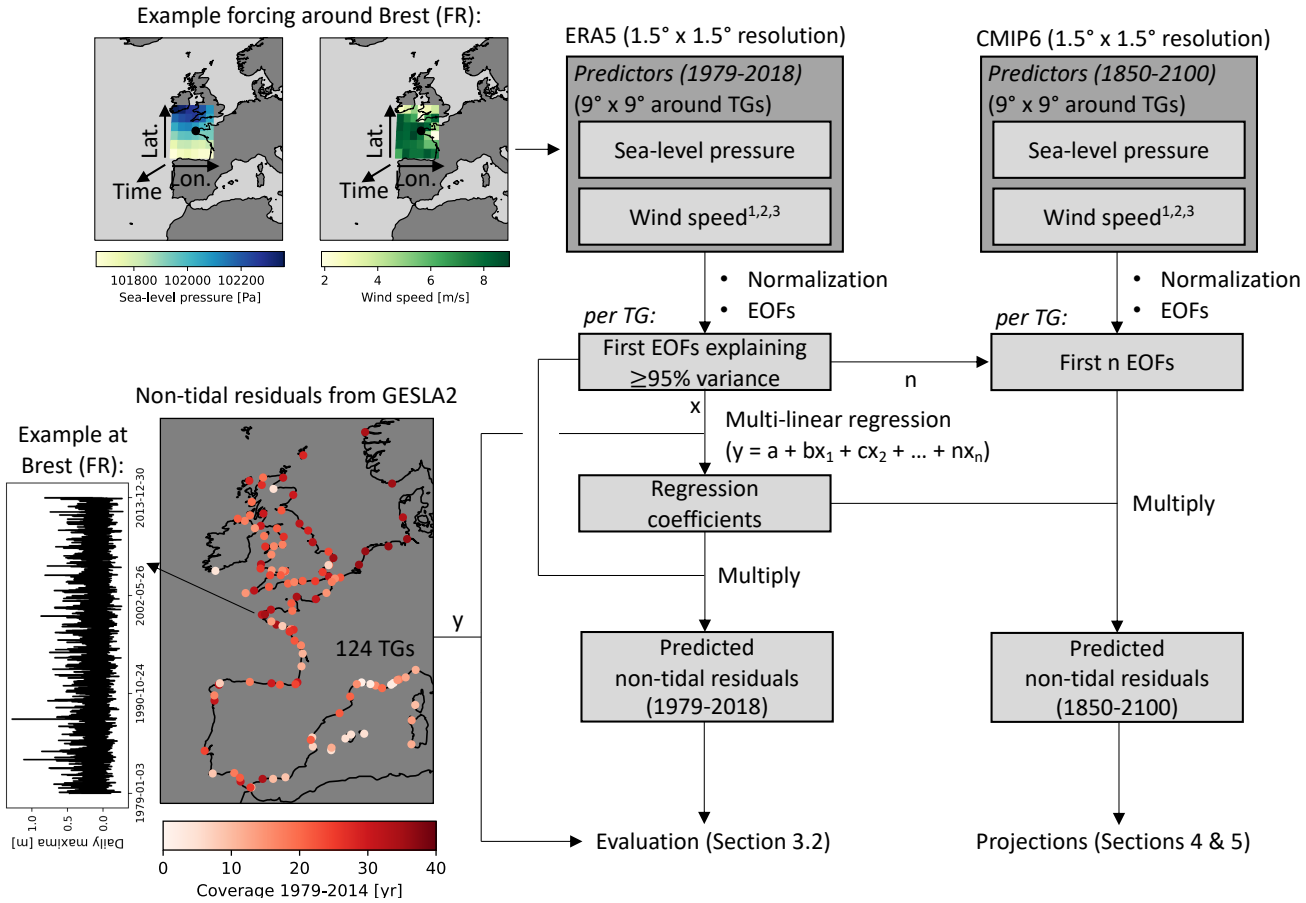

Supporting Fig. 1. Flowchart of the training of the statistical storm surge model with predictors derived from the ERA5 reanalysis (1979-2018) and predictands at tide gauges (TGs) from GESLA2 (1979-2014), and the application of the model to CMIP6 simulations (1850-2100).

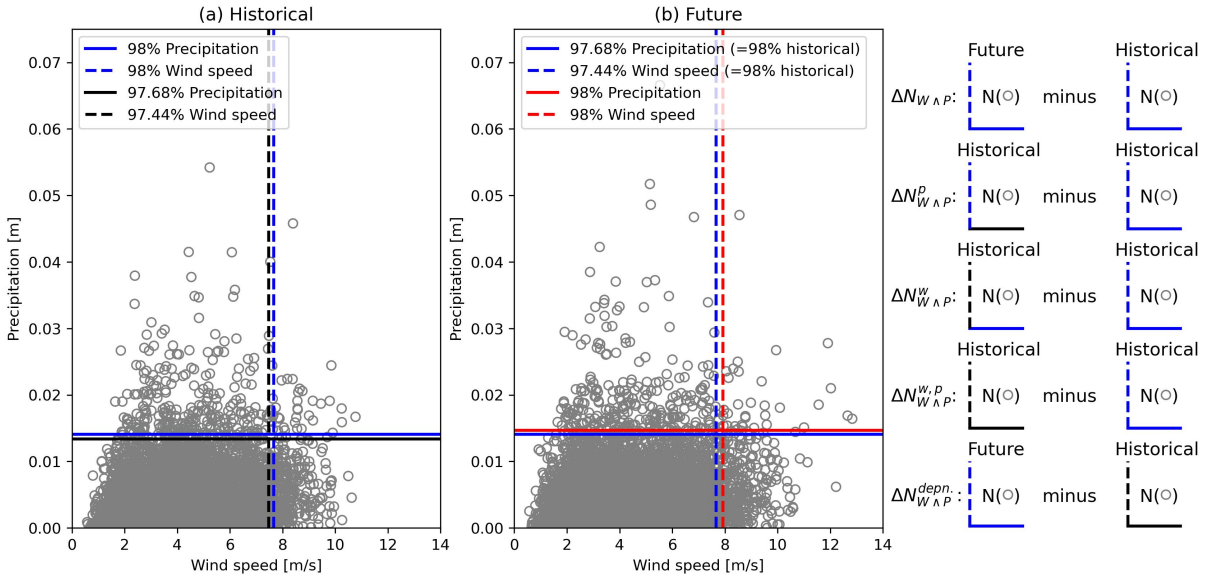

Supporting Fig. 2. Visualization of the decomposition of $\Delta N_{W \wedge P}$ at an arbitrary location for an arbitrary CMIP6 simulation. The figure shows precipitation against wind speed (grey circles) in **(a)** the historical period and **(b)** the future period. In (a), the blue solid and dashed lines indicate the 98% threshold values, and the black solid and dashed lines the 97.68% and 97.44% threshold values of precipitation and wind speed, respectively. In (b), the blue solid and dashed lines indicate the 97.68% and 97.44% threshold values, which are equal to the 98% threshold values in the historical period, and the red solid and dashed lines the 98% threshold values of future precipitation and wind speed, respectively. The right hand side of the figure shows which top-right quadrants are used to compute changes in the number of joint extremes ($\Delta N_{W \wedge P}$) due to changes in the marginal distribution of wind speed ($\Delta N^{w}_{W \wedge P}$), the marginal distribution of precipitation ($\Delta N^{p}_{W \wedge P}$), the marginal distributions of both wind speed and precipitation ($\Delta N^{w,p}_{W \wedge P}$) and the dependence between wind speed and precipitation ($\Delta N^{dependence}_{W \wedge P}$).

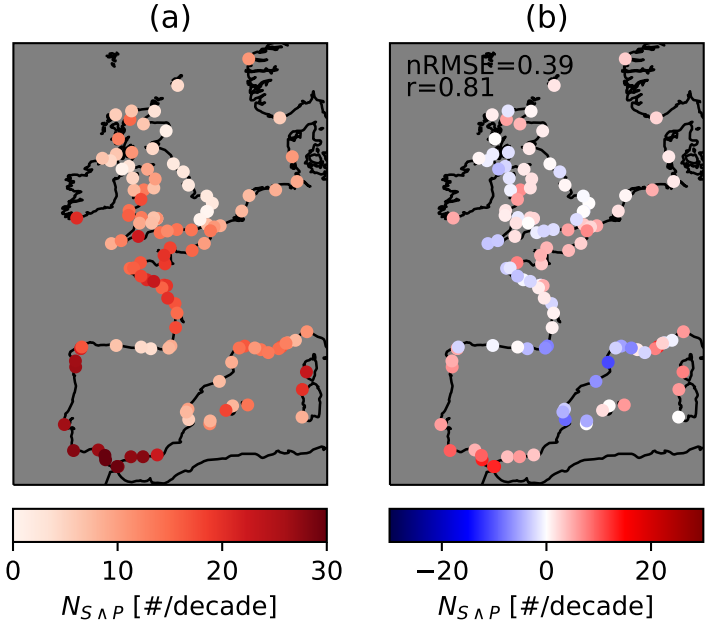

Supporting Fig. 3. **(a)** Number of joint storm surge and precipitation extremes based on storm surges computed with the statistical storm surge model trained with daily maxima from CoDEC and precipitation from ERA5, and **(b)** that number minus $N_{S_{G2} \wedge P}$. The nRMSE is normalized by dividing by the mean of $N_{S_{G2} \wedge P}$. The correlation coefficient is statistically significant ($p << 0.05$).

Supporting Fig. 4. $N^{hist}_{W\wedge P}$ simulated by individual CMIP6 models, and the multi-model ensemble mean $N^{hist}_{W\wedge P}$ (bottom right) [#/decade]. The number behind the name of each model denotes the number of initial-condition members that were used to compute $N^{hist}_{W\wedge P}$ for that model (all members available for SSP2-4.5). The emissions scenario SSP2-4.5 was used to extend the historical run to 2020.

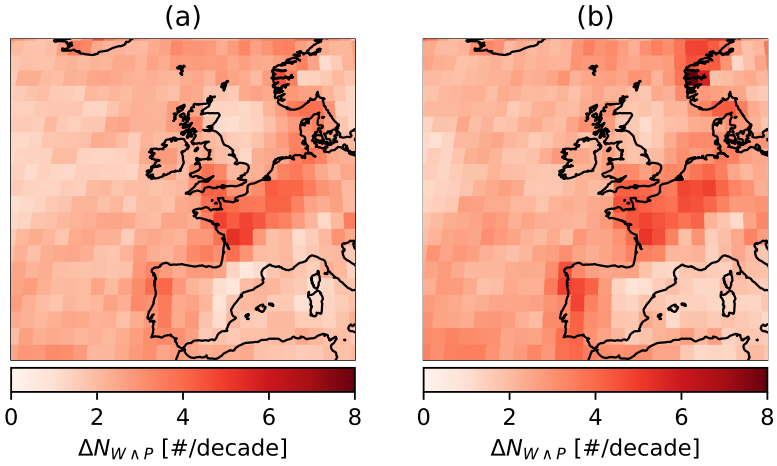

Supporting Fig. 5. CMIP6 ensemble spread (1σ) of $\Delta N_{W \wedge P}$, under **(a)** SSP2-4.5 and **(b)** SSP5-8.5, respectively.

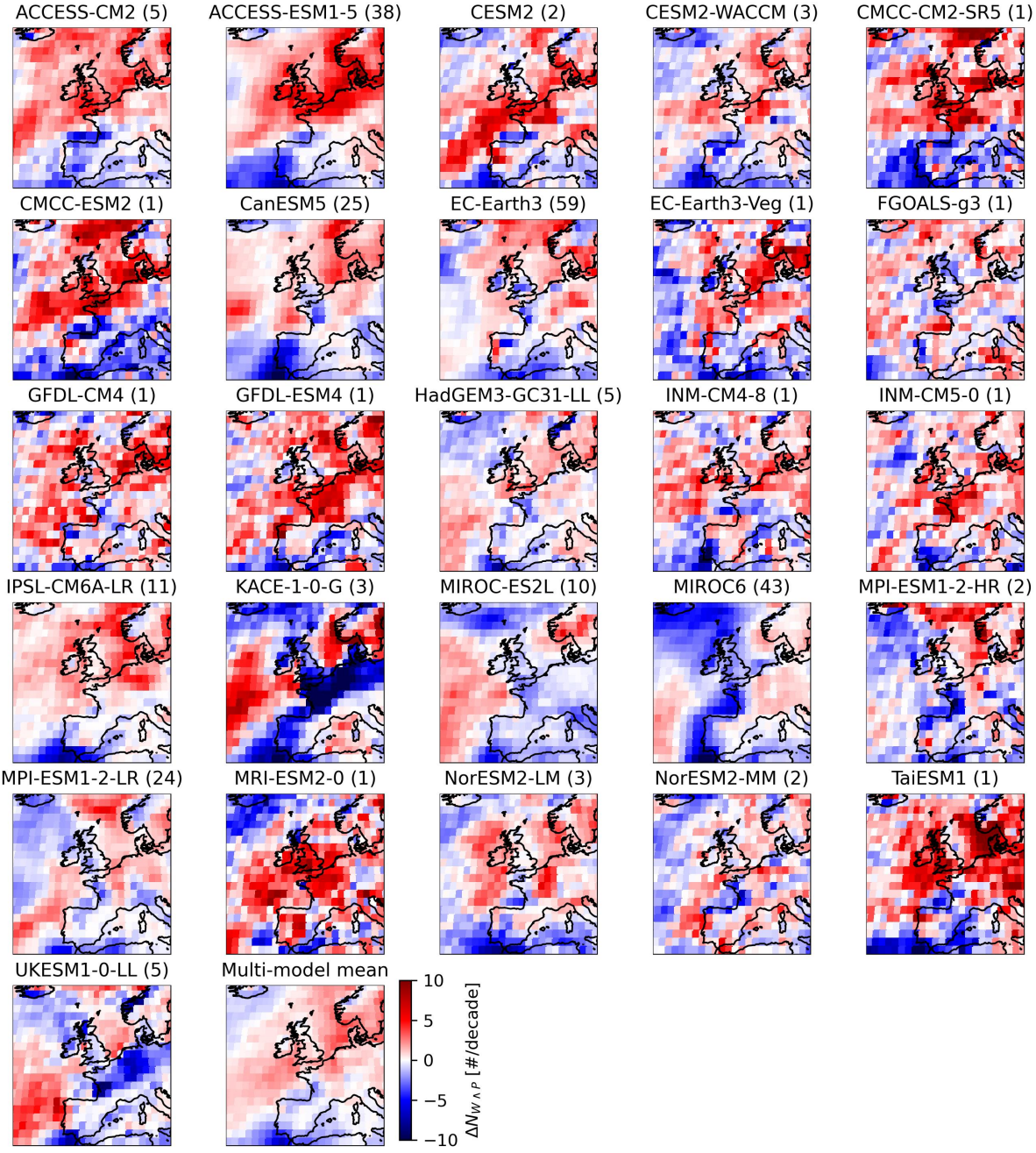

Supporting Fig. 6. $\Delta N_{W\wedge P}$ simulated by individual CMIP6 models, and the multi-model ensemble mean $\Delta N_{W\wedge P}$ (bottom right) [#/decade], under SSP2-4.5. The number behind the name of each model denotes the number of initial-condition members that were used to compute $\Delta N_{W\wedge P}$ for that model (all members available for SSP2-4.5).

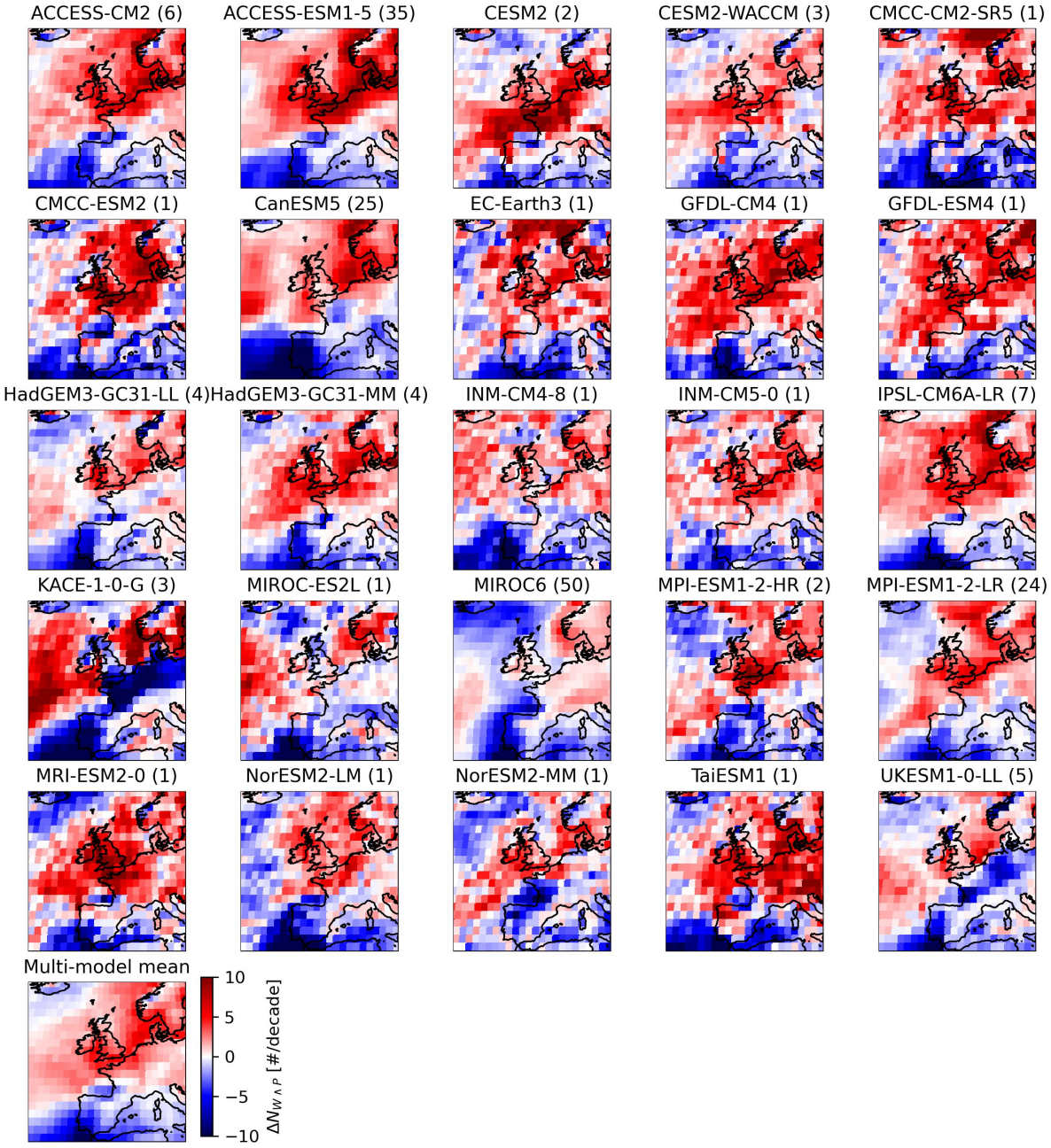

Supporting Fig. 7. $\Delta N_{W\wedge P}$ simulated by individual CMIP6 models, and the multi-model ensemble mean $\Delta N_{W\wedge P}$ (bottom right) [#/decade], under SSP5-8.5. The number behind the name of each model denotes the number of initial-condition members that were used to compute $\Delta N_{W\wedge P}$ for that model (all members available for SSP5-8.5).

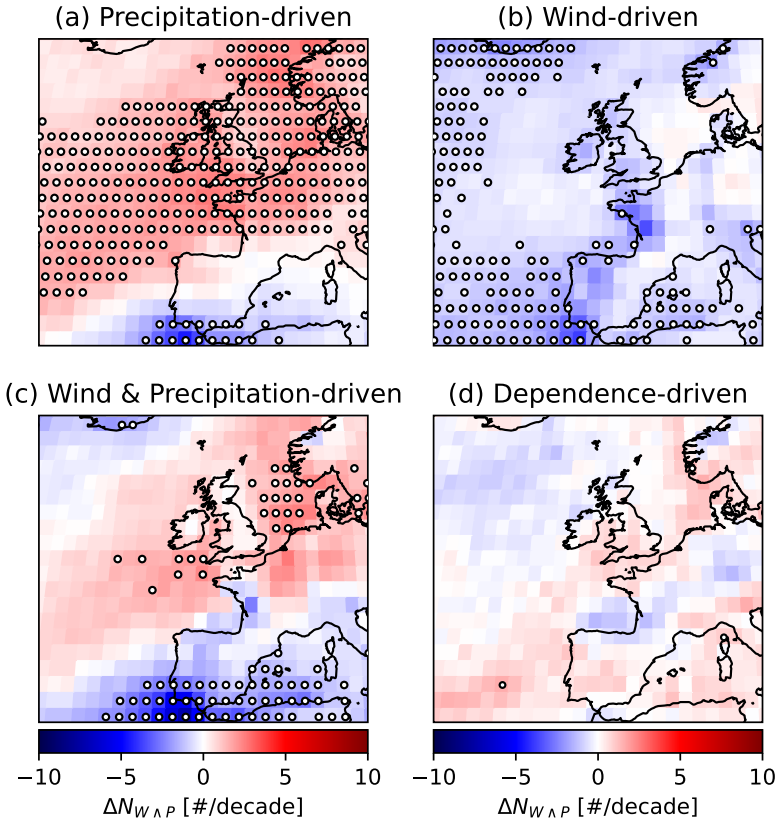

Supporting Fig. 8. CMIP6 ensemble mean $\Delta N_{W \wedge P}$ (SSP2-4.5) due to **(a)** changes in the marginal distribution of precipitation ($\Delta N^{p}_{W \wedge P}$), changes in the marginal distribution of wind speed ($\Delta N^{w}_{W \wedge P}$), changes in the marginal distributions of precipitation and wind speed together ($\Delta N^{w,p}_{W \wedge P}$), and **(d)** changes in the dependence between precipitation and wind speed ($\Delta N^{dependence}_{W \wedge P}$). The stippling indicates where the absolute value of the ensemble mean of each component of $\Delta N_{W \wedge P}$ exceeds the standard deviation of that component between models.

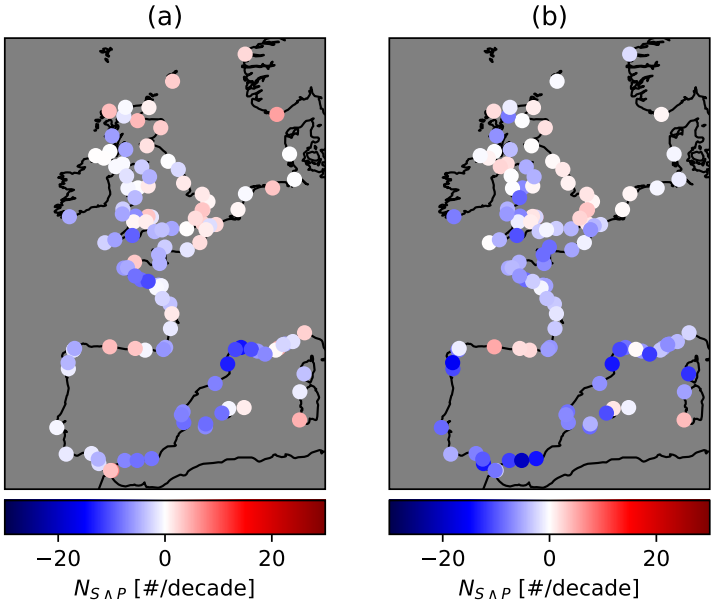

Supporting Fig. 9. (a) CMIP6 ensemble mean $N^{hist}_{S\wedge P}$ (Fig. 5a) minus $N_{SG2\wedge P}$ (Fig. 1a) and **(b)** CMIP6 ensemble mean $N^{hist}_{S\wedge P}$ (Fig. 5a) minus $N_{S_{MLR}\wedge P}$ (Fig. 1b).

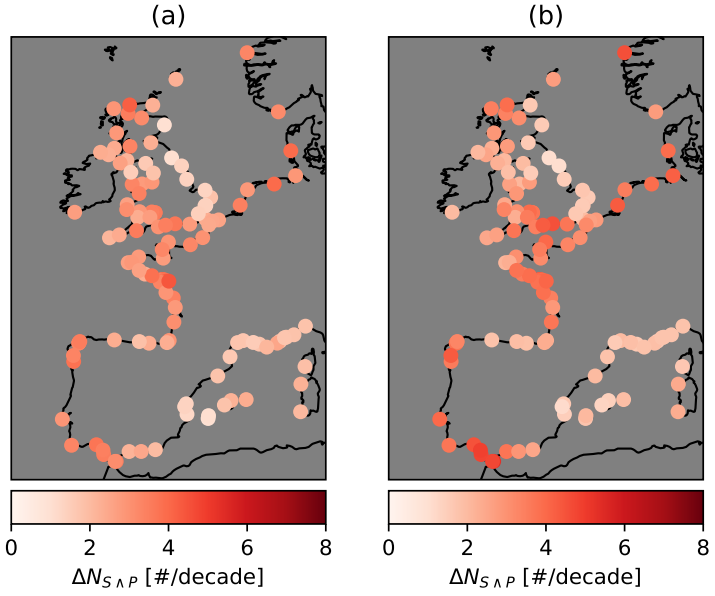

Supporting Fig. 10. CMIP6 ensemble spread (1σ) of $\Delta N_{S\wedge P}$, under **(a)** SSP2-4.5 and **(b)** SSP5-8.5, respectively.

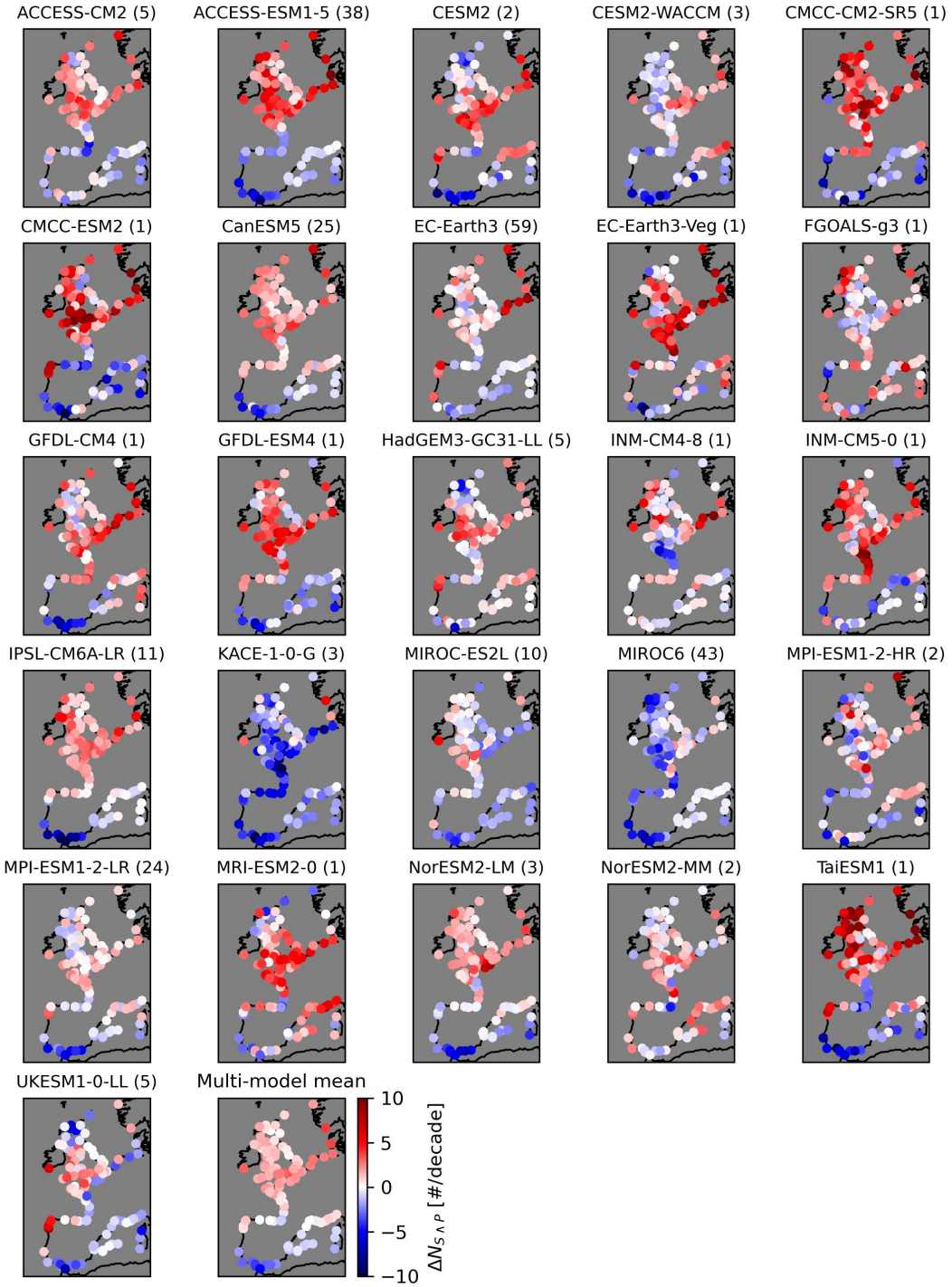

Supporting Fig. 11. $\Delta N_{S\wedge P}$ simulated by individual CMIP6 models, and the multi-model ensemble mean $\Delta N_{S\wedge P}$ (bottom right) [#/decade], under SSP2-4.5. The number behind the name of each model denotes the number of initial-condition members that were used to compute $\Delta N_{S\wedge P}$ for that model (all members available for SSP2-4.5).

Supporting Fig. 12. $\Delta N_{S\wedge P}$ simulated by individual CMIP6 models, and the multi-model ensemble mean $\Delta N_{S\wedge P}$ (bottom right) [#/decade], under SSP5-8.5. The number behind the name of each model denotes the number of initial-condition members that were used to compute $\Delta N_{S\wedge P}$ for that model (all members available for SSP5-8.5).

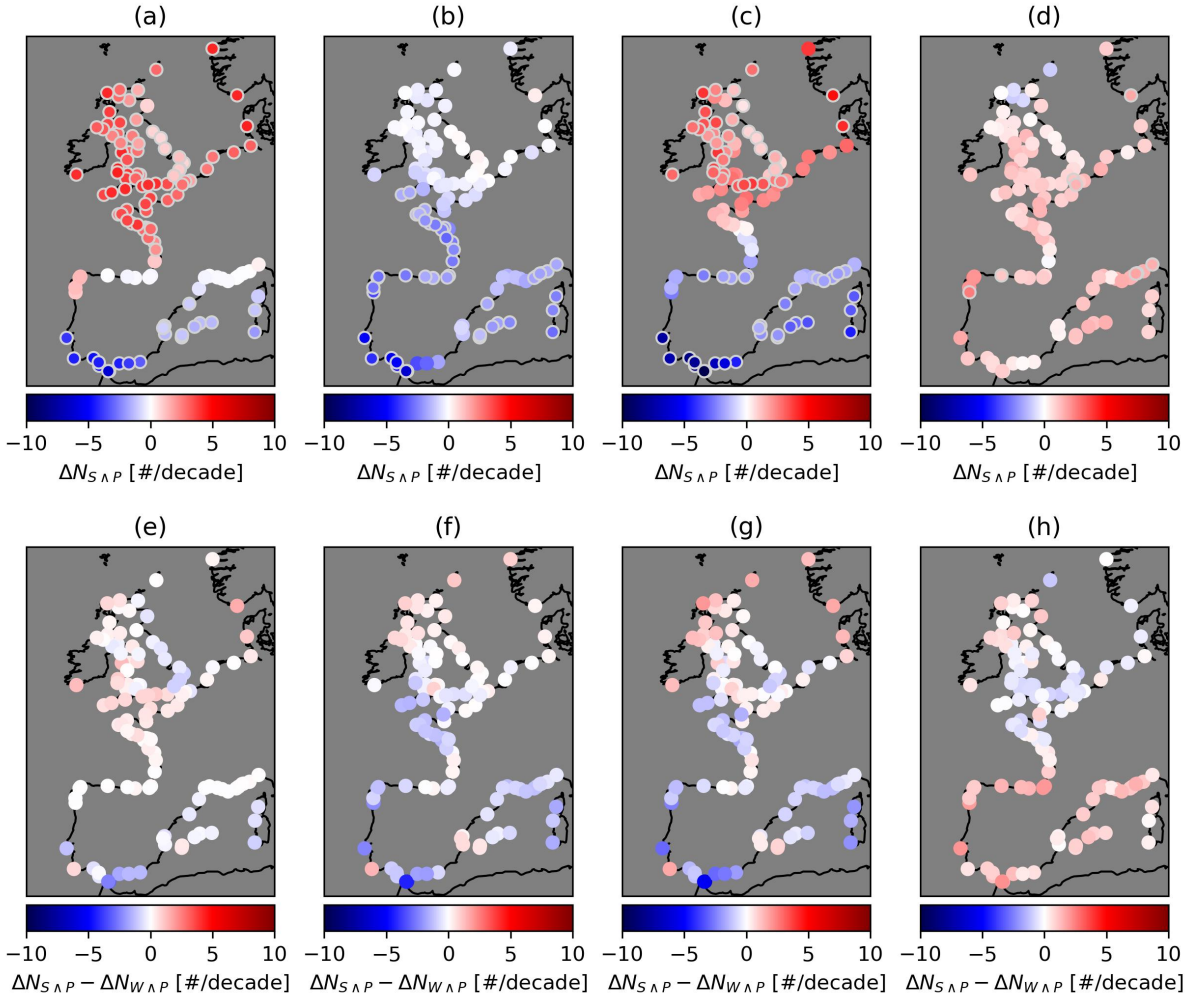

Supporting Fig. 13. CMIP6 ensemble mean of $\Delta N_{S \wedge P}$ (SSP5-8.5) due to **(a)** univariate changes in precipitation ($\Delta N^{p}_{S \wedge P}$), **(b)** univariate changes in surge ($\Delta N^{s}_{S \wedge P}$), **(c)** univariate changes in precipitation and surge ($\Delta N^{s,p}_{S \wedge P}$), and **(d)** changes in the dependence between precipitation and surge ($\Delta N^{dependence}_{S \wedge P}$); CMIP6 ensemble mean of **(e)** $\Delta N^{p}_{S \wedge P}$ minus $\Delta N^{p}_{W \wedge P}$, **(f)** $\Delta N^{s}_{S \wedge P}$ minus $\Delta N^{w}_{W \wedge P}$, **(g)** $\Delta N^{s,p}_{S \wedge P}$ minus $\Delta N^{w,p}_{W \wedge P}$ and **(h)** $\Delta N^{dependence}_{S \wedge P}$ minus $\Delta N^{dependence}_{W \wedge P}$. In (a-d), circles with a grey edge indicate where the absolute ensemble mean change exceeds the standard deviation of the change between models.

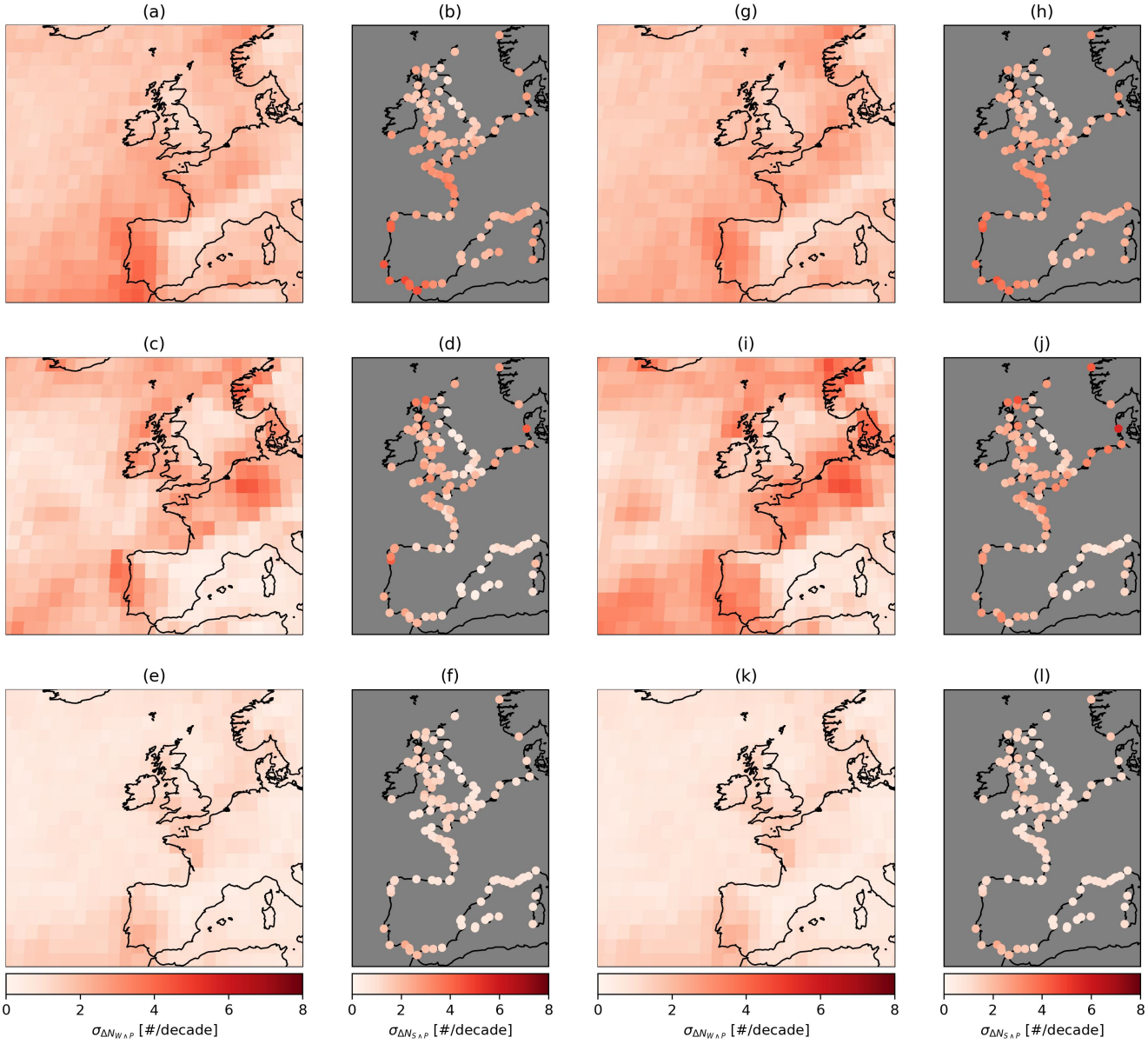

Supporting Fig. 14. Uncertainty in $\Delta N_{W\wedge P}$ and $\Delta N_{S\wedge P}$ under SSP2-4.5 due to **(a-b)** internal climate variability, **(c-d)** inter-model differences, and **(e-f)** differences between SSP2-4.5 and SSP5-8.5 [#/decade]. **(g-l)** as in (a-f), but under SSP5-8.5.

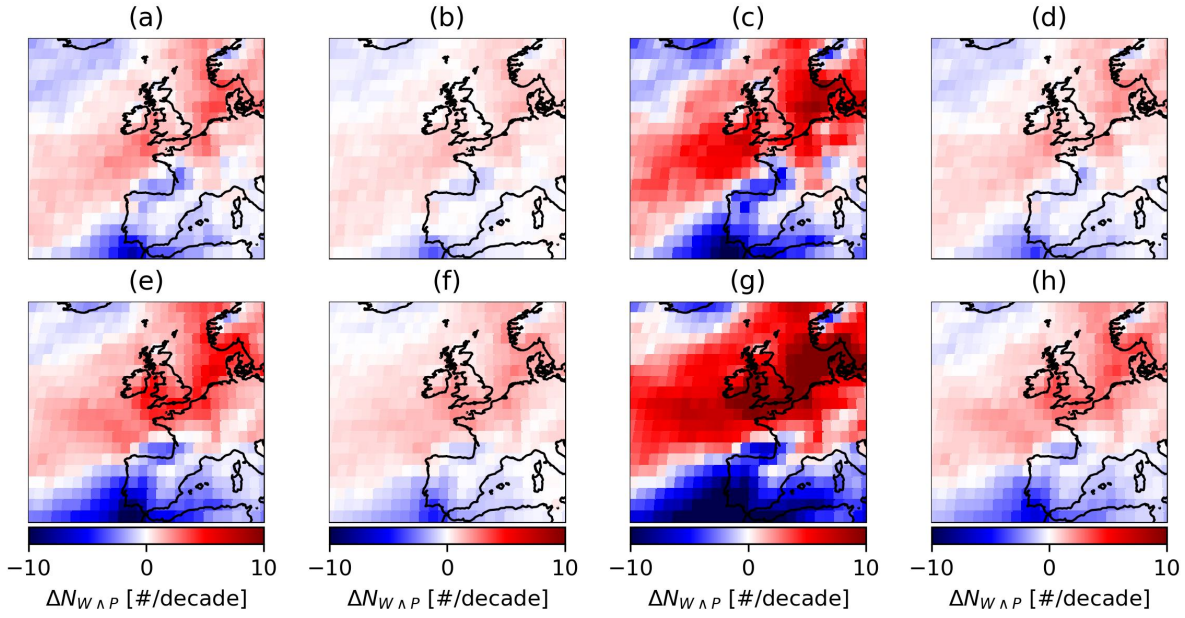

Supporting Fig. 15. CMIP6 ensemble mean $\Delta N_{W \wedge P}$ [#/decade] under SSP2-4.5 based on **(a)** the default methods described in Section 2.2, **(b)** the default methods but using the 99th percentile as the threshold for extremes, **(c)** the default methods but allowing a lag of up to two days between the extremes and **(d)** the default methods but with a 3-day declustering window applied to both extremes. **(e-h)** as in (a-d), under SSP5-8.5.

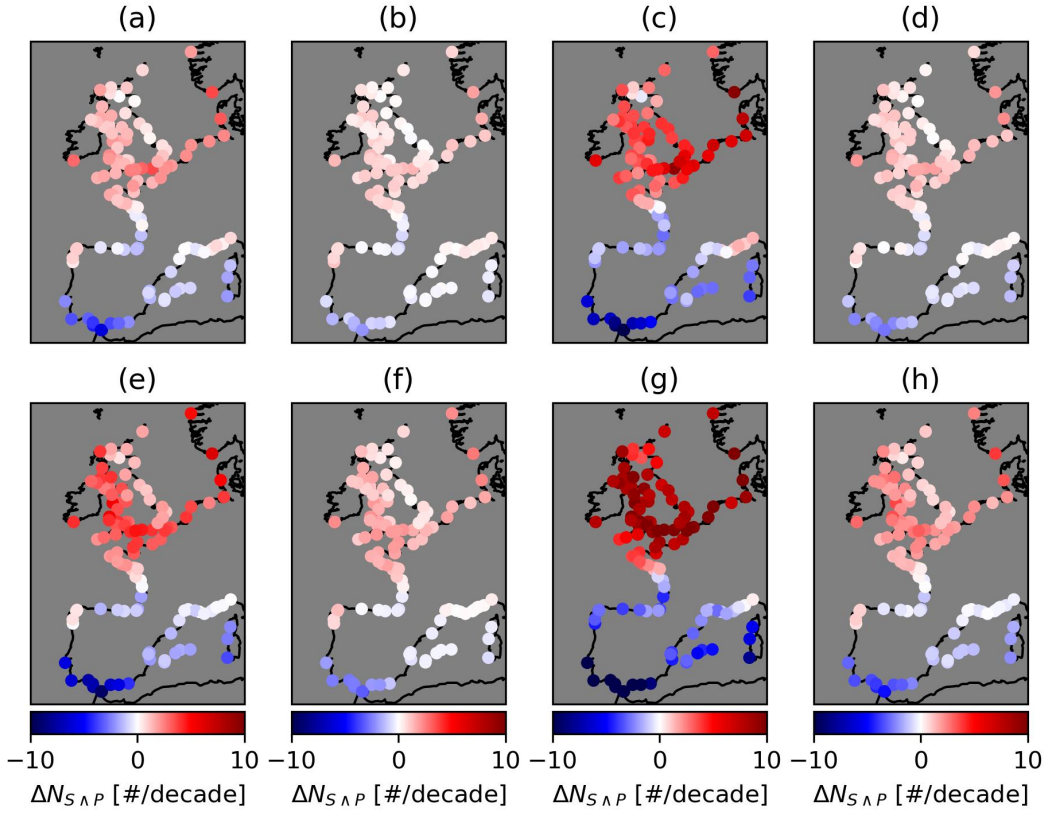

Supporting Fig. 16. CMIP6 ensemble mean $\Delta N_{S \wedge P}$ [#/decade] under SSP2-4.5 based on **(a)** the default methods described in Section 2.2, **(b)** the default methods but using the 99th percentile as the threshold for extremes, **(c)** the default methods but allowing a lag of up to two days between the extremes and **(d)** the default methods but with a 3-day declustering window applied to both extremes. **(e-h)** as in (a-d), under SSP5-8.5.